Polymer Films on Electrodes. 26. Study of Ion Transport and Electron Transfer at Polypyrrole Films by Scanning Electrochemical Microscopy

Meral Arca,† Michael V. Mirkin,‡ and Allen J. Bard*

Department of Chemistry and Biochemistry, The University of Texas at Austin, Austin, Texas 78712

Received: June 7, 1994; In Final Form: January 3, 1995®

The oxidation and reduction of the conductive polymer polypyrrole (PPy) doped with different counterions (bromide, ferrocyanide (FCN) and poly(*p*-styrenesulfonate)) was studied by scanning electrochemical microscopy (SECM) during both potential step (chronocoulometric) and cyclic voltammetric scans. The ultramicroelectrode tip was positioned close to the surface of a PPy-modified substrate electrode, and the responses of both electrodes to a substrate potential step or linear sweep were monitored simultaneously. In this way, the rates of bromide or ferrocyanide ejection during PPy reduction were shown to be functions of the reduction potential. The nature of the cation (e.g., TBA^+ vs K^+) was an important factor determining the kinetics of ion transport in the PPy^+/FCN^- films. With a solution containing TBA^+ the release of $Fe(CN)_6^{4-}$ during PPy^+/FCN^- reduction was kinetically slow, and some ferrocyanide-containing species were also ejected during film reoxidation. Direct evidence for the incorporation of cations (e.g., $Ru(NH_3)_6^{3/2+}$) in a PPy film during its reduction was also obtained by SECM measurements. Finally, the physical localization and mechanism of Fc^+ (Fc = ferrocene) and $Os(bpy)_3^{3+}$ (bpy = 2,2′-bipyridine) reduction at oxidized and reduced PPy are discussed in connection with the applicability of different models for conducting polymers.

Introduction

Charge compensation during oxidation and reduction of conducting polymers has been extensively discussed since their introduction in the late 1970s.[1] The nature of the ion transport generally cannot be deduced from the electrochemical response of the polymer-modified electrode, because it does not contribute directly to the measured current. While a number of analytical techniques, such as various electrochemical and spectroelectrochemical methods,[1−5] electrochemical quartz crystal microbalance (EQCM),[5−9] ellipsometry,[10] the bending beam method,[11] and scanning electrochemical microscopy (SECM),[12,13] have been employed to study this phenomenon, mostly qualitative and indirect information has been obtained on the relative contribution of cations and anions in the overall charge transport process. EQCM, which is one of the more powerful techniques employed in these studies,[14] suffers from a lack of selectivity, preventing an unambiguous identification of the source of the mass change (e.g., solvent motion vs cation or anion transport). Another source of ambiguity is the sensitivity of the EQCM to viscosity changes which inevitably accompany redox processes in conductive polymers. In early work, the charge compensation was assumed to be mostly due to injection and ejection of counterions.[1] Thus, for polypyrrole (PPy) and polyaniline (PANI), the cationic charge produced on oxidation was taken to be compensated by anion movement. Later, it became apparent that co-ions (i.e., cations with PPy and PANI) also participate in this process[2−4,8,9] and that the ionic transport depends significantly on the nature of both co-ions and counterions as well as on the electrode potential.[5,7,8]

The possibility of using SECM[15] by bringing an ultramicroelectrode (UME) tip close to a polymer-modified substrate electrode and monitoring selectively the flux of electroactive ions leaving or entering the film was explored by Anson and co-workers,[12] who studied ion transport of $Fe(CN)_6^{3-/4-}$ and $Os(bpy)_3^{3+/2+}$ at a Nafion/water interface. Denuault et al.[13] monitored the changes in the Cl^- concentration near a PANI-modified substrate with an ion-selective AgCl-coated SECM tip. Here we present a more quantitative approach to the study of the redox behavior of conductive polymers, based on an analysis of tip current−time ($i-t$) curves and cyclic voltammograms (CV) caused by either a step or linear sweep of the substrate potential. The expulsion of bromide and ferrocyanide anions accompanying the reduction of PPy was studied at different potentials, and direct proof of cation incorporation was obtained by the use of electroactive cations.

In the last section of the paper, we analyze SECM approach curves and cyclic voltammograms to elucidate the mechanism and physical localization of the electron transfer between redox species in solution and the PPy films. These will be discussed in connection with a choice between the porous conductor[16−19] and redox polymer[20,21] models for the polypyrrole-modified electrode. Although a number of papers have been published on this subject during the last decade, the question of the best model is still an open one.[22−27] Measurements of heterogeneous rate constants at a PPy-modified electrode will also be discussed.

Experimental Section

Chemicals. KBr (Fisher Scientific, Fair Lawn, NJ), $Ru(NH_3)_6Cl_3$ (Strem Chemicals, Newburyport, MA), K_2SO_4 (J. T. Baker, Phillisburg, NJ), tetra-*n*-butylammonium tetrafluoroborate ($TBABF_4$, 99%), sodium poly(*p*-styrenesulfonate) (MW ~ 70 000, Aldrich Chemical Co, Milwaukee, WI), $K_4Fe(CN)_6$ (Merck, Rahway, NJ), and acetonitrile (Burdick and Jackson, Muskegon, MI) were used as received. Tris(2,2′-bipyridyl)-osmium(II) ($Os(bpy)_3^{2+}$) was synthesized according to previously reported procedures.[28] Pyrrole (Aldrich) was distilled under vacuum and stored under argon atmosphere at low temperature. Aqueous solutions were prepared with deionized water (Milli-Q, Millipore Corp.). Ferrocene (Fluka Chemical Corp., Ronkonkoma, NY) was sublimed twice before use.

† Permanent address: Hecettepe University, Chemistry Department, 06532, Beytepe, Ankara, Turkey.

‡ Present address: Department of Chemistry and Biochemistry, Queens College−CUNY, Flushing, NY 11367.

® Abstract published in *Advance ACS Abstracts,* March 15, 1995.

0022-3654/95/2099-5040$09.00/0

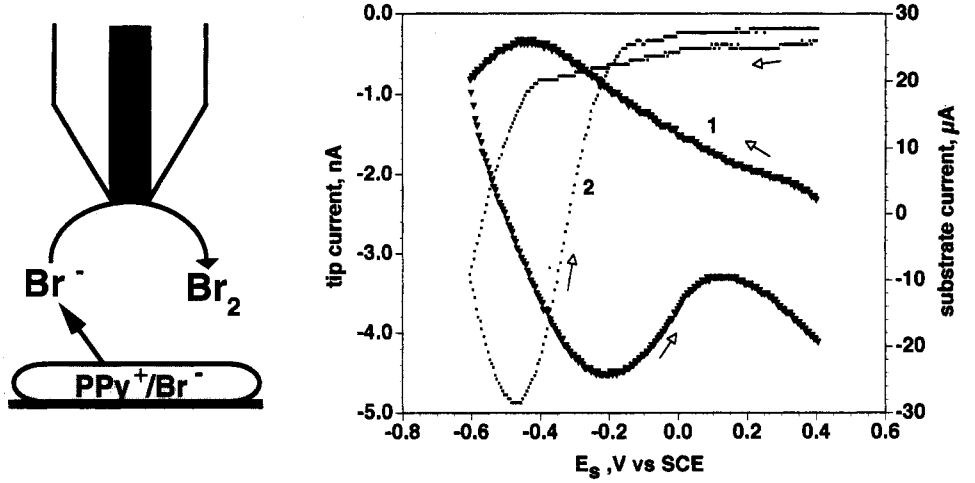

Figure 1. SECM substrate cyclic voltammogram of PPy^+/Br^- in 0.1 M K_2SO_4 solution and corresponding dependence of tip current vs substrate potential. Polypyrrole was electropolymerized at +0.75 V vs SCE in a solution containing Br^- counterions. The tip–substrate distance, d, was about 5 μm. (1) Voltammogram of 1-mm-diameter Pt substrate modified with a 10 μm-thick PPy^+Br^- film. Cathodic scan started at +0.4 V. ν = 10 mV/s (2) Tip current as a function of substrate potential. The 25-μm-diameter Pt tip was held at +0.9 V vs SCE where Br^- is oxidized.

Electrodes. The 25-, 10-, and 2-μm-diameter Pt microdisk tips were fabricated as described previously[29] and were polished with 0.05-μm alumina before each experiment. SECM measurements were performed in a 3-mL Teflon cell. Data were acquired with either a three- or a four-electrode configuration: with a Pt wire serving as a counterelectrode, with an SCE (in aqueous solutions) or a Ag wire (in acetonitrile) as a reference electrode, and with the substrate electrode either biased or unbiased. A 1-mm-diameter Pt wire (Johnson Matthey, Seabrook, NH) was sealed in glass, polished with 0.05-μm alumina, and used as a substrate for the electrodeposition of polypyrrole. The SECM apparatus was described previously.[30] A PAR (Princeton Applied Research, Princeton, NJ) Model 175 programmer was used to generate potential steps in transient measurements. The approach curves and $i-t$ transients were obtained with an EI-400 four-electrode potentiostat (Ensman Instruments, Bloomington, IN).

Preparation of PPy Films. For experiments in aqueous solutions, PPy films (0.5- to 10-μm-thick) loaded with Br^- counterions, PPy^+/Br^-, were prepared using a BAS-100A electrochemical analyzer (Bioanalytical Systems, West Lafayette, IN) in the bulk electrolysis mode by potentiostatic oxidation of 0.1 M pyrrole at a Pt anode at either +0.75 or +1.0 V vs SCE in an aqueous solution containing 0.2 M KBr. A small amount of oxidation of Br^- may occur during preparations at +1.0 V until the PPy^+/Br^- film builds up to a thickness where the oxidation of Br^- at Pt is diminished. Polypyrrole/ferricyanide (PPy^+/FCN^-) films were prepared in the same manner, with the polymerization carried out at 0.75 V in aqueous 0.1 M pyrrole and 0.1 M $K_4Fe(CN)_6$.[31] The electrochemical polymerization of polypyrrole/poly(*p*-styrenesulfonate) (PPy^+/PSS^-) was carried out at +0.75 V in aqueous solution containing 0.1 M pyrrole and 0.2 M sodium poly(*p*-styrenesulfonate).[4] The PPy^+/BF_4^- films for nonaqueous experiments were prepared by potentiostatic oxidation of 0.1 M pyrrole at a Pt electrode at +1.1 V vs Ag QRE (corresponding to about 0.9 V vs a Ag/AgCl reference electrode) in acetonitrile solution containing 0.2 M $TBABF_4$. The resulting modified electrodes were rinsed with MeCN and heated for 2 h at 80 °C.

SECM Procedure. Monitoring of ion expulsion from PPy films was carried out during either cyclic voltammetry or chronocoulometry experiments. In both cases, the UME tip (either a 10- or 25-μm-diameter Pt disk) was positioned close to the film/solution interface. To avoid possible interference of an added redox couple with the PPy electrochemistry in ejection monitoring experiments, we chose to use dissolved oxygen as a mediator to achieve precise tip positioning, as described previously.[32] In voltammetric experiments the PPy-modified substrate potential (E_S) was scanned between +0.4 and −0.6 V vs SCE, the tip potential (E_T) was held at E_T = +0.9 V, and both the tip and substrate currents were monitored simultaneously. In chronocoulometric trials, the E_S was stepped from the initial value, +0.5 V vs SCE, to 0, −0.2, or −0.6 V, while E_T was held at +0.9 V for Br^- monitoring. In cation ejection experiments, E_S was stepped from 0 V vs SCE to +0.5 V with E_T = −0.45 V to reduce $Ru(NH_3)_6^{3+}$. The tip and substrate current transients caused by such potential steps were recorded and then integrated numerically to determine the amount of charge passed. Tip and substrate cyclic voltammograms of Fc^+ and $Os(bpy)_3^{3+}$ reduction at PPy were obtained in a similar way, with E_T chosen to be sufficiently negative for the reduction process to be diffusion controlled. Note that in all curves cathodic currents are indicated and plotted as positive values and anodic currents as negative values.

Results and Discussion

Ionic Transport during Redox Cycling of Polypyrrole. During the polymerization of pyrrole, supporting electrolyte anions (e.g., Br^-) were incorporated into the PPy film.

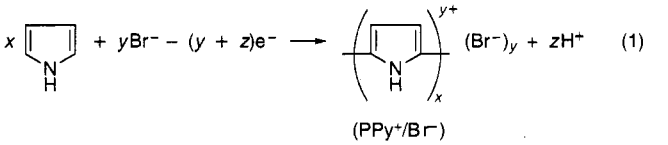

The PPy^+/Br^- film was transferred to the SECM cell containing an inert electrolyte solution (e.g., K_2SO_4) and the nature of the ion ejection and incorporation processes during PPy^+/Br^- reduction and PPy reoxidation was studied. A typical cyclic voltammogram of the substrate covered with a 10-μm-thick PPy film loaded initially with bromide counterions (curve 1) is shown in Figure 1 along with the simultaneously recorded dependence of the tip current upon substrate potential (curve 2). The 25-μm-diameter Pt tip, located ~5 μm from the film, was biased at +0.9 V vs SCE, where bromide oxidation is diffusion controlled, so the tip current reflects the flux of Br^- ions ejected from the PPy^+/Br^- and arriving at the tip surface. Comparison of curves 1 and 2 reveals a wide potential range (roughly from +0.1 to −0.3 V vs SCE) where the reduction of

PPy^+ is accompanied by almost no expulsion of bromide. Bromide ion is detected at potentials more negative than −0.3 V and continues on scan reversal as long as cathodic current flows. The Br^- oxidation current decreases during PPy oxidation (E_S > −0.5 V) because Br^- diffuses into the bulk solution and some is taken up in the PPy film.

Two possible explanations can be proposed for the delayed Br^- response: either there is some time delay in the tip response because of slow bromide diffusion and migration in the polymer (the bromide diffusion between the film and tip electrode in solution takes less than 1 ms for a tip−substrate separation on the order of 1 μm[33]) or cation incorporation, rather than anion expulsion, occurs in this potential region. To check for the possibility of a time delay in anion expulsion, we carried out time-of-flight SECM experiments as described previously.[33] A short (ms) potential pulse from +0.5 to −0.6 V vs SCE was applied to the initially oxidized PPy substrate, leading to substrate reduction and tip oxidation (E_T = 0.9 V vs SCE) current transients. The time delay between the substrate and tip transients represents the time required for bromide ions to diffuse to the tip surface. Unlike the results with a AgBr film,[33] where a time delay on the order of 1 s was detected and attributed to the ion diffusion through a micrometer-thick AgBr layer, in the present case, the delay was clearly negligible on the time scale of Figure 1. This result also suggests that the reduction of PPy begins at the film/solution interface rather than at the Pt/PPy boundary, in agreement with previous ellipsometric results.[10] Thus, the difference between the onset of PPy^+ reduction and Br^- oxidation at the tip is caused by a substantial dependence of the bromide expulsion rate upon reduction potential.

The results suggest that both cation incorporation (eq 2) and anion expulsion (eq 3) occur during film reduction, i.e.,

$$PPy^+/Br^- + e^- + K^+ \rightarrow PPy\ K^+Br^- \quad (2)$$

$$PPy^+/Br^- + e^- \rightarrow PPy + Br^- \quad (3)$$

A quantitative description of the above phenomenon is not straightforward because no comprehensive theory is available for polypyrrole switching and for the associated ion transport. To study the extent of anion ejection as a function of reduction potential, we performed generation/collection measurements under identical experimental conditions varying only the magnitude of the substrate potential step. Before each measurement, the same 10-μm-diameter Pt tip was positioned at approximately the same distance (about 5 μm) from the 10-μm-thick freshly polymerized oxidized PPy^+/Br^- film. After the application of a potential step to the substrate, the long-time (20 s) tip and substrate current transients (Figure 2) were acquired and the amount of charge passed was calculated by numerical integration of each curve. The integral collection efficiency (g) was the most suitable parameter to characterize the amount of ejected material. This parameter, taken as $g = Q_T A_S/Q_S A_T$, where Q_T and Q_S are total amounts of charge for the tip and substrate processes, respectively, and A_T and A_S are the surface areas for each electrode (i.e., the amount of charge collected at the tip electrode normalized by the amount of charge passed at an equivalent area on the substrate surface), remained essentially constant for a given magnitude of the potential step, although the magnitudes of Q_T and Q_S were not so reproducible. Table 1 contains the results obtained for three different values of the reduction potential: −0.6, −0.2, and 0.0 V vs SCE. A value of g = 1.5 at −0.6 V was obtained for the complete reduction of PPy, as expected because of the convergent diffusion to the UME tip. The results indicate that anion transport is primarily responsible for maintaining electroneutrality when the potential is stepped to a sufficiently negative value. However, the effective collection efficiency decreased dramatically at more positive reduction potentials (i.e., −0.2 or 0.0 V), suggesting that significant cation incorporation into the PPy film occurs at the less negative potentials. This is in contrast with the results of other authors[4,8] who observed that anion motion predominated during the oxidation of PPy films prepared with small anions.

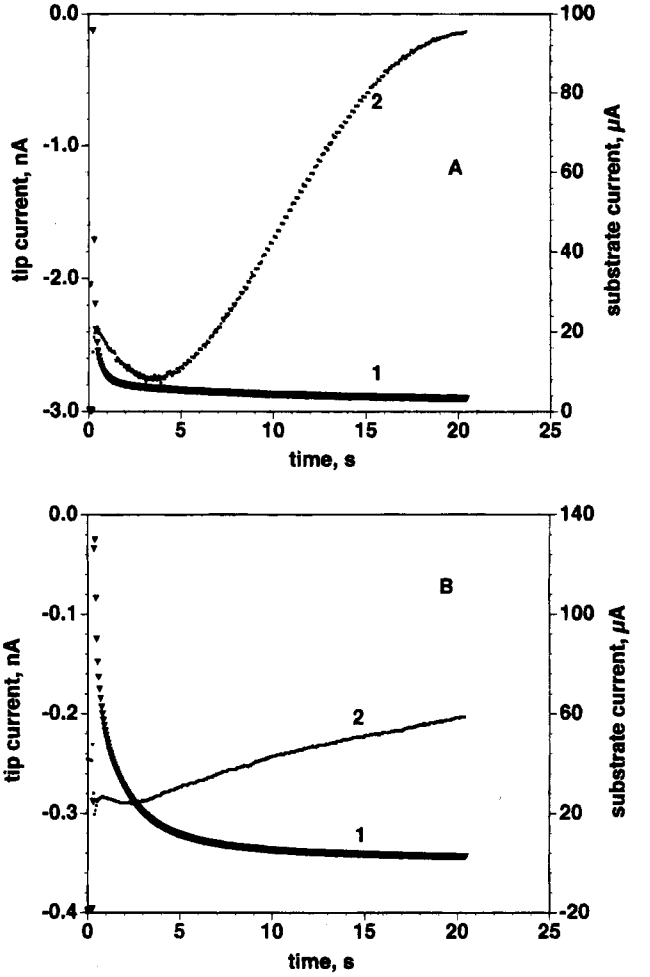

Figure 2. Substrate (1) and tip (2) current−time curves obtained after the application of a potential step to the PPy^+Br^--modified substrate electrode. The potential step was (A) from +0.5 to −0.6 V and (B) from +0.5 to 0.0 V vs SCE, and the tip recorded Br^- oxidation. a = 5 μm. For other parameters, see Figure 1. Note, however, the difference in tip current scales in A and B. The tip current spikes observed immediately after the potential step application are caused by capacitive coupling between the electrodes.[29]

TABLE 1: Effective Collection Efficiency ($g = Q_T A_S/Q_S A_T$) of Bromide Ions at a 10-μm-Diameter Pt Tip Electrode Following the Reduction Potential Step at a PPy-Coated 1-mm-Diameter Pt Substrate

potential step from/to V vs SCE	$Q_T \times 10^8$ C	$Q_S \times 10^4$ C	g	average g for the given potential step
0.5/−0.6	11.0	7.6	1.42	1.5
0.5/−0.6	11.0	11.0	1.00	
0.5/−0.6	11.0	5.3	2.10	
0.5/−0.2	0.66	1.3	0.50	0.56
0.5/−0.2	2.4	3.9	0.61	
0.5/0.0	0.77	2.6	0.29	0.33
0.5/0.0	0.48	1.8	0.27	
0.5/0.0	1.2	3.6	0.33	
0.5/0.0	1.1	2.7	0.41	

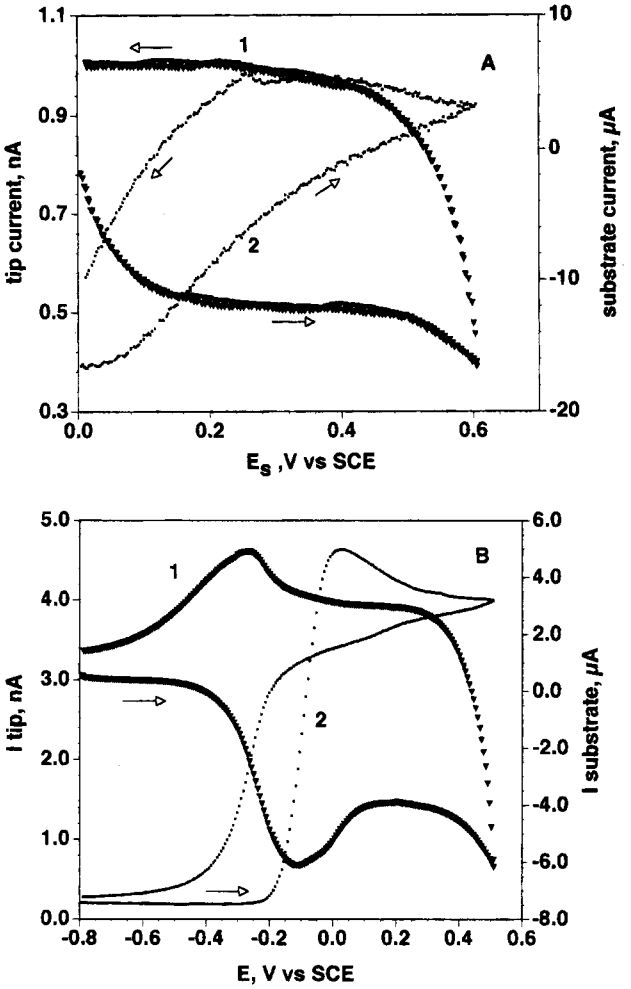

Figure 3. SECM substrate (1) and tip (2) cyclic voltammograms of PPy films (initially containing $Ru(NH_3)_6^{3+}$ (A) or $Ru(NH_3)_6^{2+}$ (B)) in 0.1 M K_2SO_4 solution. (A) PPy film prepared at +0.75 V vs SCE in solution containing 0.2 M KBr and then partially reduced at 0.0 V vs SCE in a solution containing 0.1 M $Ru(NH_3)_6^{3+}$. (B) PPy film prepared at +0.8 V vs SCE in solution containing 0.2 M sodium poly(*p*-styrenesulfonate) and then reduced at −0.8 V vs SCE in a solution containing 0.1 M $Ru(NH_3)_6^{3+}$. The tip current is due to reduction of $Ru(NH_3)_6^{3+}$ ejected from PPy. $E_T = -0.45$ V. $v = 10$ mV/s.

To obtain direct evidence for cation incorporation during reduction, we partially reduced PPy^+/Br^- (potential step from +0.5 to 0.0 V) in a solution containing an electroactive cation, 0.1 M $Ru(NH_3)_6^{3+}$

$$PPy^+/Br^- + e^- + {}^1/_3Ru(NH_3)_6^{3+} \rightarrow PPy[Ru(NH_3)_6^{3+}]_{1/3}Br^- \quad (4)$$

The resulting film was rinsed and used as the SECM substrate, as described above. The Pt tip in this experiment was biased at −0.45 V vs SCE to observe the diffusion-controlled reduction of $Ru(NH_3)_6^{3+}$ at the tip rather than the oxidation of bromide. The resulting oxidation scan CV (Figure 3A) and chronoamperograms (Figure 4) showed cathodic tip currents attributed to $Ru(NH_3)_6^{3+}$ reduction and demonstrated that during partial reduction PPy incorporated a considerable amount of $Ru(NH_3)_6^{3+}$. This effect is even greater for PPy films doped with poly(styrenesulfonate) (PPy^+/PSS^-), because these large polyanions are bound more strongly to the polymer matrix and cation transport dominates.[4,21] Curve 2 in Figure 3B compared to the analogous dependence in Figure 3A indeed shows an about 4−5 times higher peak current for $Ru(NH_3)_6^{3+}$ reduction and a lower

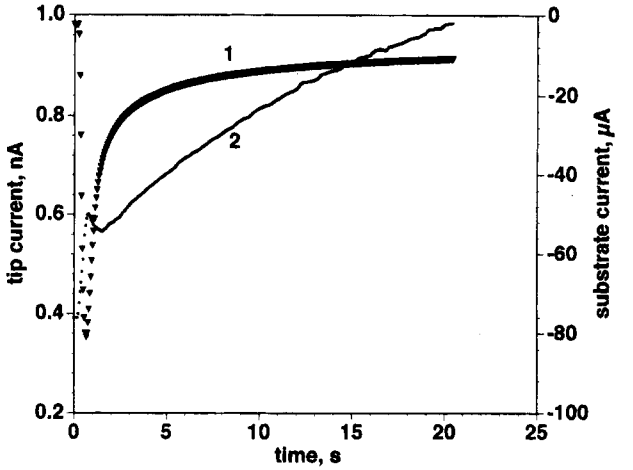

Figure 4. Substrate (1) and tip (2) current−time curves for a PPy^+Br^- film containing $Ru(NH_3)_6^{3+}$. $E_T = -0.45$ V. The potential step was from 0.0 to +0.6 V vs SCE, and the tip recorded $Ru(NH_3)_6^{3+}$ reduction. The film prehistory was the same as in Figure 3A. At short times, the substrate current grows with time due to the increase in PPy conductivity.[25,34]

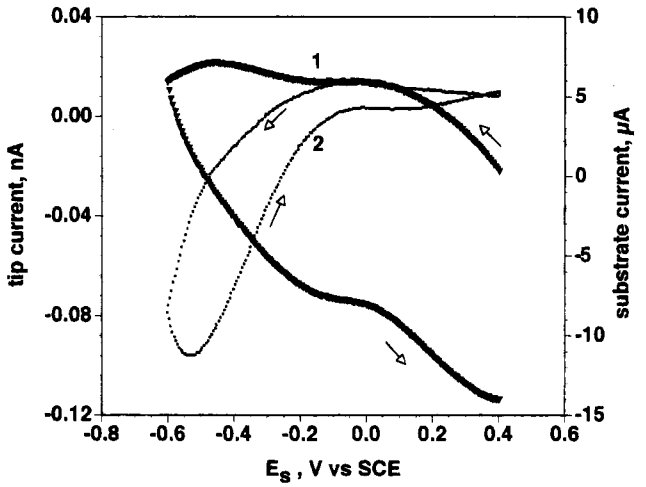

Figure 5. Same as Figure 1, but PPy prepared at +1.0 V vs SCE. $a = 5$ μm.

substrate current (curve 1), demonstrating that extensive cation incorporation occurred during the reduction of PPy^+/PSS^- at a potential as negative as −0.8 V vs SCE.

$$PPy^+/PSS^- + {}^3/_2e^- + {}^1/_2Ru(NH_3)_6^{3+} \rightarrow PPy[Ru(NH_3)_6^{2+}]_{1/2}PSS^- \quad (5)$$

This is in contrast with the behavior of PPy^+/Br^- films which predominantly eject anions when reduced at negative potentials.

Many authors have reported a pronounced dependence of the morphology and properties of PPy upon the polymerization potential.[1,35] For example, Heinze and Bilger[9] deduced from EQCM measurements that the relative contributions of anions and cations to the overall charge transport for PPy^+/ClO_4^- in propylene carbonate depended strongly on the potential of the film preparation (e.g., +0.7 vs +1.0 V vs Ag/AgCl). We also investigated possible changes in cation and anion transport associated with the film prehistory. However, PPy^+/Br^- films prepared at +0.85 and +1.0 V vs SCE (Figure 5) showed essentially the same behavior as those polymerized at +0.75, i.e., almost no Br^- ejection at $E \leq -0.2$ V and significant ejection at more negative potentials.

One can deduce from the above experiments that incorporation of cations (either K^+ or $Ru(NH_3)_6^{3+}$) at $E \leq 0.2$ V vs SCE

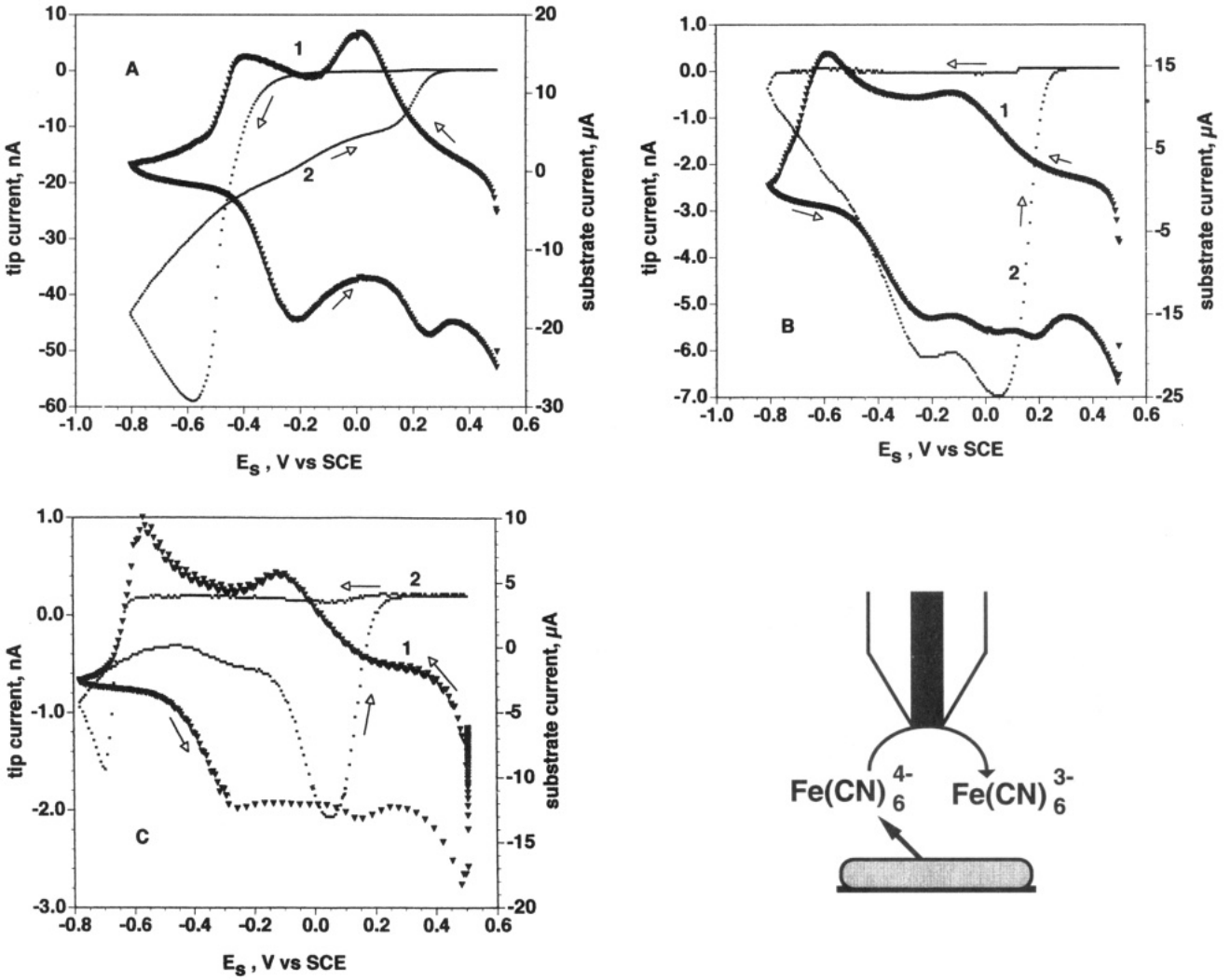

Figure 6. Substrate CV of PPy^+/FCN^- (1) and corresponding dependencies of tip current vs substrate potential (2). Supporting electrolyte was (A) 0.1 M K_2SO_4 and (B) 0.1 M TEACl. $v = 10$ mV/s. $a = 5$ μm, (C) Same as B, but $v = 5$ mV/s. The film thickness was about 2 μm (calculated from the polymerization charge[31]). $E_T = +0.5$ V where $Fe(CN)_6^{4-}$ oxidation occurs. Other parameters are as in Figure 1.

is energetically preferable to ejection of Br^- from PPy^+/Br^-, while at more negative potentials anion ejection becomes favorable. This potential dependent behavioral difference may be connected with either polymer morphology changes or water ejection from the film, which could decrease its solvating ability. The alternative explanation is that the film just accepts as many cations as it can and only then does anion ejection begin; this could explain why anions are not expelled at less negative potentials, where the extent of PPy reduction is lower. However, this model is not in accord with potential step experiments, where the tip transients obtained at $E = -0.6$ V (Figure 2A) do not show any time delay.

The substrate CV of initially oxidized PPy^+/FCN^- obtained in 0.1 M K_2SO_4 solution (Figure 6A, curve 1) shows two cathodic and, on reversal, two anodic peaks. The first pair of peaks (corresponding to $E^{o\prime} = 0.1$ V vs SCE) is due to reduction of $Fe(CN)_6^{3-}$ moieties incorporated into the film and oxidation of $Fe(CN)_6^{4-}$. The second pair of peaks at more negative potentials is caused by the PPy^+/PPy redox reaction. Charge compensation for both reductions could be achieved by either expulsion of $Fe(CN)_6^{4-}$ or incorporation of K^+ ions. The flat base line of the tip voltammogram (Figure 6A, curve 2) on the cathodic scan shows that no appreciable ejection of ferrocyanide occurs at substrate potentials more positive than −0.3 V vs SCE. This finding is in agreement with previous results obtained by pulse measurements in a special small-volume cell with three working electrodes[36] and by generation/collection flow technique.[5b] This lack of loss of $Fe(CN)_6^{4-}$ is probably due to the strong affinity of the multicharged anion for the oxidized PPy film. Very similar CVs were obtained with a 0.1 M solution of Na_2SO_4 or KCl. The picture is completely different for PPy^+/FCN^- films in 0.1 M tetraethylammonium chloride (TEACl) solution (Figure 6B). From the well-reproducible dependence of the tip current vs substrate potential (curve 2) one can see that no ejection of $Fe(CN)_6^{4-}$ occurs until E_S becomes as negative as −0.7 V. This can be attributed to a greater affinity of TEA^+ for PPy compared to that of K^+. Surprisingly, ejection of ferrocyanide occurs during the oxidation of PPy when the opposite process (i.e., anion injection) is expected. The replacement of chloride anions with sulfate did not affect this experiment in any significant way. The two distinct peaks on a tip voltammogram may correspond to different kinds of ejected species. One possible reason for this behavior could be a very sluggish expulsion of $Fe(CN)_6^{4-}$ from the PPy film. If this is the case, a decrease in the potential sweep rate should lead to significant peak displacement on the tip voltammogram. Such a change can indeed be seen in Figure 6C; at $v = 5$ mV/s, the first of the two peaks in the tip voltammogram is displaced and now occurs, as expected, during the cathodic substrate scan. This portion of the tip voltammogram looks, in fact, similar to curve 2 in Figure 6A. The second peak, however, does not displace at all with the change in v. Although we do not have

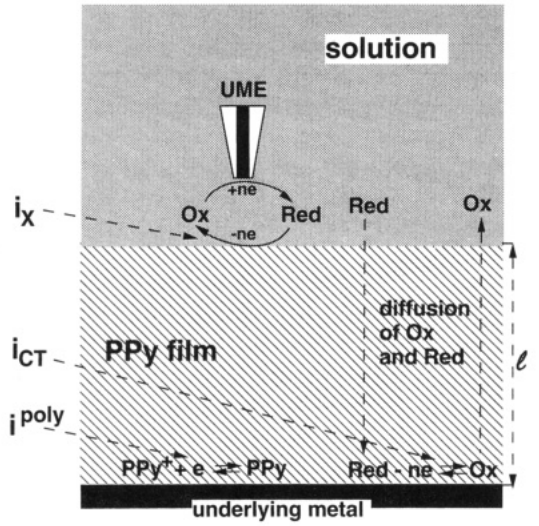

Figure 7. Processes at a PPy-modified electrode. Different components of a PPy-modified SECM substrate current (i_S) are associated with polypyrrole redox reaction, i^{poly}, direct oxidation/reduction of redox species at the underlying metal electrode, i_{CT}, and redox reaction at a PPy/solution interface, i_X (cf. eq 6; i_{DL} is not shown). At $l \gtrsim a$ the tip current reflects only the last process.

a satisfactory explanation for the details of the behavior, the association of TEA^+ with $Fe(CN)_6^{4-}$ ions and the ejection of the complex cationic or neutral species $[TEA_nFe(CN)_6]^{+n-4}$ during PPy oxidation might occur.

Electron Transfer between PPy Films and Redox Couples in Solution. Here we aim to answer two questions about electron transfer (et) reactions of solution species at a PPy-modified electrode: (i) where does et occur (i.e., at the substrate/film or at the film/solution interface or within the PPy layer) and (ii) what are the mechanisms of the interfacial redox reaction at both oxidized and reduced PPy? There are very different answers to these questions in the recent literature, reflecting either a porous conductor model[16-19] or a redox polymer model.[20-22] The main difference between these two models is the assumption of electronic conductivity (i.e., a delocalized band structure) in the first case versus localization of the charge in the polymer chain and an electron-hopping conductivity mechanism in the second. Doblhofer[22] recently presented a consistent account of the latter model, and we use his terminology to discuss the applicability of this concept to heterogeneous et at oxidized and reduced PPy. The total electric current at a PPy modified electrode is[22]

$$i_S = i_{DL} + i^{poly} + i_{CT} + i_X \qquad (6)$$

where i_{DL} is the double-layer charging current, i^{poly} is the current associated with PPy oxidation/reduction ($PPy^+ + e = PPy$), i_{CT} is the current due to oxidation (or reduction) of the electroactive species at the underlying metal electrode, and i_X represents chemical reaction between the polymer and mediator:

$$Red + PPy^+ = Ox + PPy \qquad (7)$$

where Ox and Red are oxidized and reduced forms of the mediator. Equations 6 and 7 indicate that oxidation/reduction of the solution redox species may proceed either via et at the underlying metal electrode (penetrating through pores in the PPy layer[17]) or via chemical reaction with PPy. Figure 7 represents the above scheme (i_{DL} is not shown), assuming that the reduced form of electroactive species is oxidized at a PPy-modified SECM substrate.

The rate of reaction 5 is[22]

$$i_X = FAk_X \int_0^l c_{P+}(x)\, c_{Red}(x)\, dx \qquad (8)$$

where A is the substrate surface area, k_X is the bimolecular rate constant, and $c_{P+}(x)$ and $c_{Red}(x)$ are concentrations of PPy^+ and Red within the film. The potential dependence of i_X arises only from the c_{P+} term, and thus, it is associated with the oxidation and reduction of PPy rather than with any specific redox couple in solution. This is analogous to the situation in electrochemical reactions at semiconductors, where the voltammetric potentials are related to the band edge positions rather than to the E° of the redox mediator.[37] One should note that Figure 7 and eq 6 would apply to the porous conductor model as well. The i_X term in that case corresponds to the electrochemical oxidation or reduction of a mediator at the film/solution interface,

$$Red - e^- \rightleftharpoons Ox \qquad (9)$$

which is expected to occur at a potential characteristic for a given redox couple and to follow Butler−Volmer kinetics.

To elucidate the physical location of the et reaction and the rate-limiting stage of the interfacial process, we apply the previously formulated diagnostic criteria[33] to the SECM approach curves. In such curves a redox mediator, e.g., $Os(bpy)_3^{2+}$, is introduced in solution and oxidized at the tip electrode (to $Os(bpy)_3^{3+}$). Reaction of $Os(bpy)_3^{3+}$ at the substrate produces a flux of $Os(bpy)_3^{2+}$ back to the tip, causing the tip current to be larger than that observed when the tip is far from the substrate. The magnitude of this positive feedback effect depends upon the tip−substrate spacing and the rate of reaction of the tip-generated species at the substrate. Approach curves were obtained with two different redox mediators, i.e., ferrocene (Fc) (Figure 8) and $Os(bpy)_3^{2+}$ (Figure 9) over a PPy film substrate. In these experiments, a reactant (i.e., Fc^+ or $Os(bpy)_3^{3+}$) is generated at the Pt tip, and the feedback current from its reaction at the PPy substrate provides information about the nature of the reaction at PPy. These approach curves (i.e., I_T vs L dependencies, where $I_T = i_T(d)/i_{T,\infty}$ is the normalized tip current corresponding to a tip−substrate separation d; $i_{T,\infty} = 4nFDc^*a$ is the tip current at an infinite tip−substrate distance; and $L = d/a$) were obtained with Pt tip electrodes of two different sizes ($a = 1\ \mu$m, Figures 8A and 9A,D,E, and $a = 5\ \mu$m, Figures 8B−E and 9B,C) and also with different thicknesses of the PPy films at several potentials. A positive feedback current ($I_T > 1$) was observed in all experiments, and the maximum attainable normalized current, $I_{T,max}$, ranged from 1.8 to about 3. Attempts to bring the tip closer to the substrate led to a tip current increase by many orders of magnitude, signaling direct contact between the two electrodes. The uncertainty in the zero-separation point found in this way was about $\pm 0.1\ \mu$m. The smallest $I_{T,max}$ value obtained, 1.8 (Figure 8A), would correspond to an effective tip−substrate separation, d/a, of about 0.8 for diffusion-controlled mediator turnover. Since the film thickness, $l = 10\ \mu$m, was 10 times the tip radius, the contribution of direct reduction of Fc^+ at the Pt substrate (i.e., i_{CT} in eq 6 and in Figure 7) to I_T was negligible. Thus, the mediator regeneration occurs at the film-solution interface or within the PPy film, but not at the Pt/PPy boundary. The same result can be deduced from the approach curves obtained with the $Os(bpy)_3^{2+}$ mediator (Figure 9). Thus, most of the electroactive species do not penetrate the thick (1−10 μm) PPy film and react at the underlying Pt, in contrast to earlier work with thinner films.[16,17]

A common feature of all of the approach curves in Figures 8 and 9 is the much lower values of the feedback current at

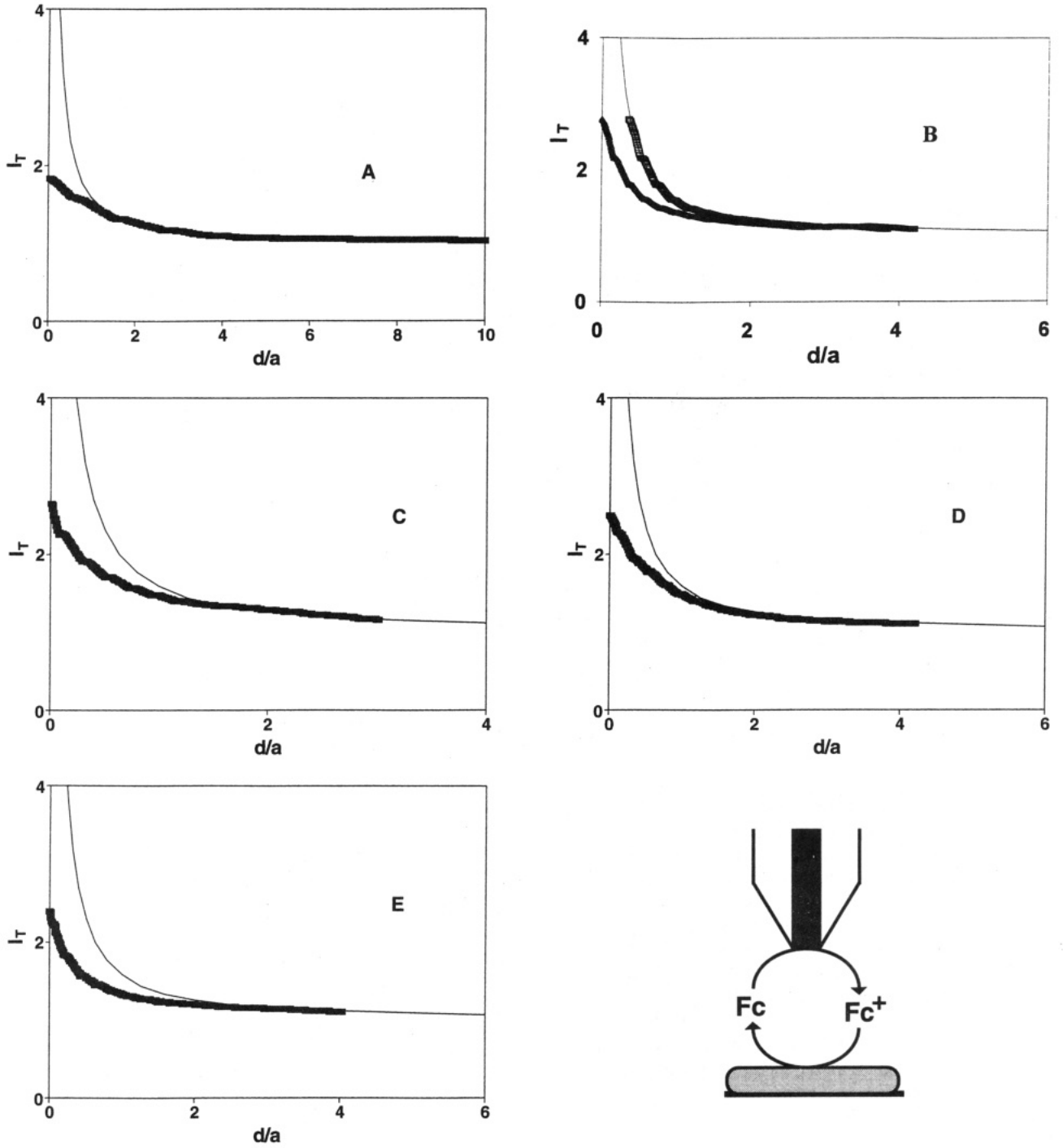

Figure 8. Current−distance curves for a Pt tip approaching PPy^+/BF_4^- in acetonitrile solution with Fc mediator (5 mM Fc and 0.1 M in $TBABF_4$). The tip potential was kept sufficiently positive, so the oxidation of Fc was diffusion controlled. The film thickness (l), tip radius (a), and substrate potential vs Ag QRE (E_S) were as follows: (A) $a = 1$ μm, $l = 10$ μm, $E_S = 0.2$ V; (B) $a = 5$ μm, $l = 10$ μm, $E_S = 0.2$ V; (C) $a = 5$ μm, $l = 1$ μm, $E_S = 0.2$ V; (D) $a = 5$ μm, $l = 10$ μm, unbiased oxidized PPy film; (E) $a = 5$ μm, $l = 10$ μm, unbiased PPy^+/BF_4^- film completely reduced before measurements. Thin solid curves represent the theory for a diffusion-controlled process and a planar conductive substrate;[38] thick lines represent experimental data. (B) Open squares: same current−distance curve, but with 1.8 μm offset.

small tip−substrate distances compared to a diffusion-controlled process in SECM with a conductive substrate[38] (thin solid curves in all figures). Possible reasons for such behavior include (1) significant roughness of the PPy film, preventing the tip from coming close to the substrate, (2) regeneration of the redox mediator occurring within the film rather than at the solution interface, and (3) slow heterogeneous kinetics. The last possibility can be excluded by analysis of I_T−L curves obtained with tips of different size. Equation 10 describes the SECM current−distance curve with finite heterogeneous kinetics at the substrate.[33]

$$I_T^k = \frac{I_T}{(1 + 1/\Lambda_c)} + \frac{I'}{(1 + \Lambda_c)} \tag{10}$$

where I_T^k is the normalized tip current under kinetic control, $I' = 0.68 + 0.3315 \exp(-1.0672/L)$, $\Lambda_c = kd/D$ (where k is the heterogeneous chemical or electrochemical rate constant and D is the diffusion coefficient), and the normalized diffusion-controlled tip current is

$$I_T = 0.78377/L + 0.3315 \exp(-1.0672/L) + 0.68 \tag{11}$$

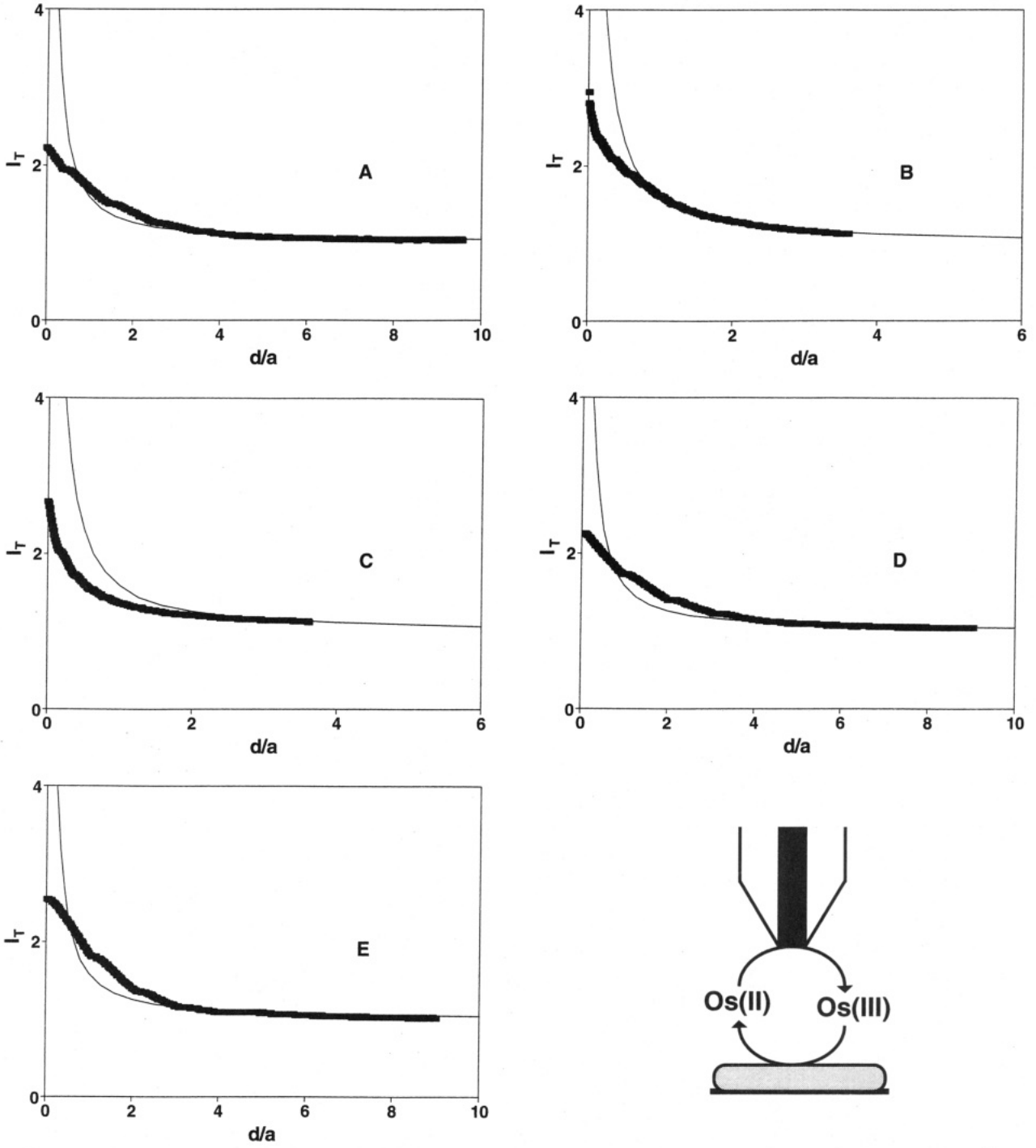

Figure 9. Current−distance curves for a Pt tip approaching PPy^+/BF_4^- in aqueous solution with $Os(bpy)_3^{2+}$ mediator (5 mM $Os(bpy)_3^{2+}$ and 0.5 M KNO_3). The tip potential was kept sufficiently positive, so the oxidation of $Os(bpy)_3^{2+}$ was diffusion controlled. The film thickness (l), tip radius (a), and substrate potential vs SCE (E_S) were as follows: (A) $a = 1$ μm, $l = 10$ μm, $E_S = 0.2$ V; (B) $a = 5$ μm, $l = 10$ μm, $E_S = 0.2$ V; (C) $a = 5$ μm, $l = 1$ μm, $E_S = 0.2$ V; (D) $a = 1$ μm, $l = 10$ μm, unbiased oxidized PPy substrate; (E) same as D, but with reduced PPy biased at −0.45 V. Thin solid curves represent the theory for a diffusion-controlled process and a planar conductive substrate;[38] thick lines represent experimental data.

From eq 10, the expression for the maximum kinetically limited normalized tip current at $d \rightarrow 0$ is

$$I_{T,max}^{k} = \lim_{d \to 0} I_T^{k} = \frac{\pi k a}{4D} \tag{12}$$

According to eq 12, under kinetic control, $I_{T,max}$ should be proportional to the tip radius. A comparison of the approach curves in Figure 8A,B shows only about a 20% increase in $I_{T,max}$ when a was changed by a factor of 5 (from 1 to 5 μm). The analogous increase in $I_{T,max}$ in Figure 9A,B is about 25%. Thus, the substrate process is not controlled by heterogeneous kinetics. The same conclusion can be drawn from approach curves obtained at thinner (i.e., 1-μm-thick) films.

Since the PPy film is rough, e.g., small fibers of PPy stick out into the solution, electric contact between the tip and PPy occurs as the tip approaches the main polymer/solution interface. Thus, the apparent zero-separation point on the current−distance curve obtained by the large current rise does not coincide with the coordinate of the actual (average) film/solution boundary, and the experimental $I_T - L$ curve can be fitted to the theory by introduction of some "offset", i.e., by displacement of the zero-

separation point (open squares in Figure 8B). This effect does not change significantly the shape of the I_T-L curve. In contrast to the above, the regeneration of the mediator within the PPy layer (as opposed to the regeneration at the film/solution interface) should affect dramatically the shape of I_T-L curves when the depth of ion penetration is comparable with the tip radius.[33] The deviation of the experimental current−distance curve from the theory in this latter case cannot be corrected by introduction of any offset. Such a distortion of the approach curves is clearly seen in Figures 8A and 9A, showing that the thickness of the reaction layer inside the PPy film is comparable with the tip radius (1 μm). The current−distance curves obtained with a 5-μm-radius tip are not distorted, and the exact fit with the theory can always be achieved with an offset value of 1.5−2 μm (this fit is shown in Figure 8B; all other I_T-L curves obtained with $a = 5$ μm can be treated similarly). This result and also the lack of difference between the curves obtained at 1- and 10-μm-thick PPy films (curves B and C in Figures 8 and 9) suggest that the reaction layer thickness inside the PPy film for both mediators is probably less than 1 μm (otherwise these approach curves would be different). The offset values of about 2 μm thus reflect the combined effect of the film roughness and the ion penetration into the porous PPy.

Two other approach curves (Figures 8D and 9D) were obtained with a 5-μm-radius tip approaching a 10-μm-thick PPy film. In both cases, the substrate was unbiased and the PPy was used as prepared in the oxidized state. The positive feedback current in both curves can result either from the chemical reaction (eq 7) (according to the redox polymer model) or from the electrochemical reaction (eq 9) (if PPy behaves as a metal whose open circuit potential is determined by solution redox species). The first explanation implies that the concentration of reduced moieties in oxidized PPy is sufficiently high to support chemical regeneration of a mediator at a diffusion-controlled rate. If so, the I_T-E_S curves in Figure 10A,B would show a significant fraction of a potential-independent residual current due to chemical reaction between PPy and oxidized species in solution, which is not the case. Apparently, the concentration of the reduced moieties in oxidized PPy is so low that the chemical reaction is much slower than the electrochemical one. Thus, the reduction of both Fc^+ and $Os(bpy)_3^{3+}$ at oxidized PPy seems to follow an electrochemical mechanism. These two processes occur at significantly different potentials characteristic of the specific redox reaction rather than for oxidation/reduction of PPy, which remained oxidized over the whole potential sweep range. Both processes display near-reversible Butler−Volmer-type kinetics, and their I_T-E_S curves correspond to conventional electrochemical theory (see below). All these findings are compatible only with a model that assumes extensive charge delocalization in oxidized PPy.

Surprisingly, the approach curves obtained with either unbiased (Figure 8E) or biased (at −0.45 V vs SCE, Figure 9E), reduced, highly resistive, PPy are very similar to that obtained at an oxidized, conductive, PPy. Again, a 10-μm-thick film was much too thick for mediator regeneration at the Pt surface. The electrochemical mechanism of mediator regeneration is implausible here because of the very low conductivity of reduced PPy (e.g., 10^{-7} S cm^{-1} in 0.1 M $TEAClO_4$/MeCN[39]). From Figure 10C, one can see that I_T is essentially independent of substrate potential over the range of E_S from 0 to −0.9 V vs SCE, although the PPy conductivity decreases dramatically over the same range.[39] All of these findings are consistent with the chemical regeneration of a mediator via reaction 7. From the analysis of I_T-L curves, the kinetics of both chemical reactions appear to be rapid. The lower limits for apparent heterogeneous

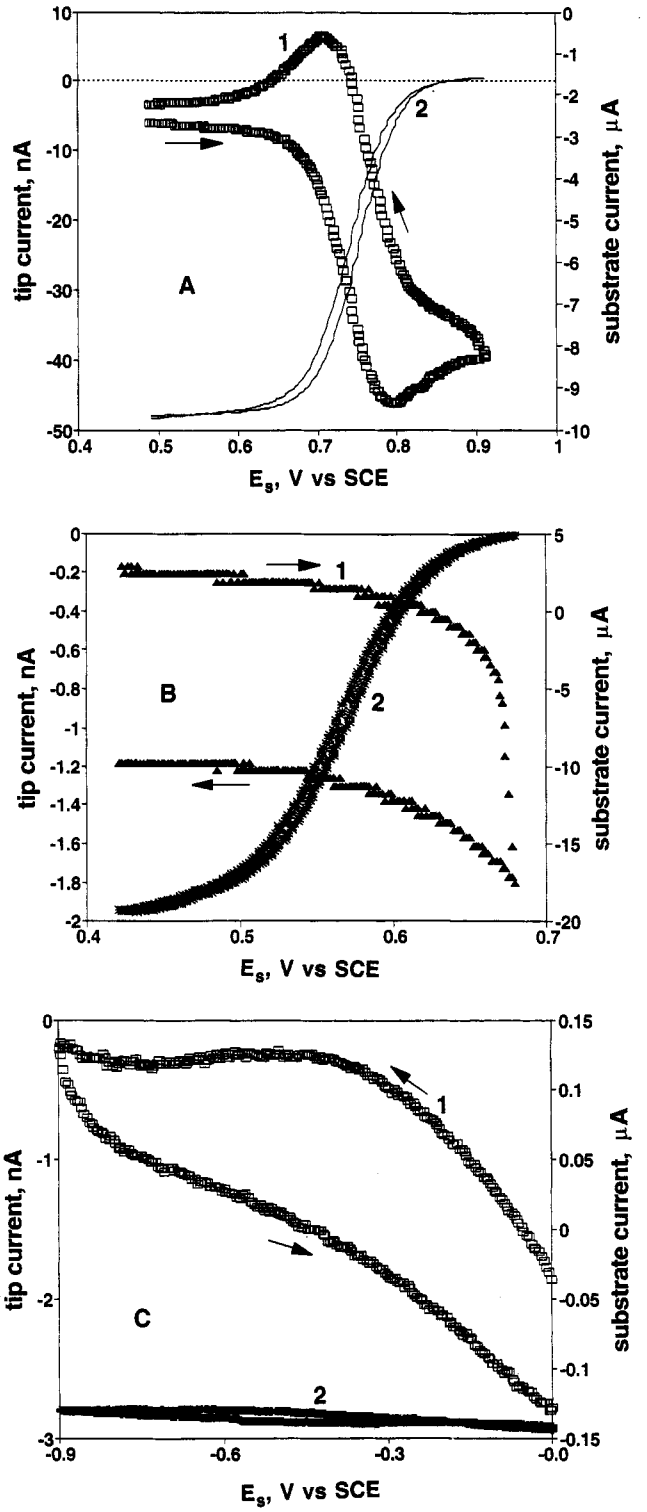

Figure 10. Voltammograms (i_S-E_S (1) and i_T-E_S (2)) of the reduction of (A) Fc^+ on PPy^+/BF_4^- in acetonitrile and (B and C) $Os(bpy)_3^{3+}$ in aqueous solution. $a = 5$ μm. v = (A) 20, (B) 10, and (C) 10 mV/s. The tip was positioned as close to the substrate as possible without contacting the PPy film. Solution composition and film thickness were (A) 5 mM Fc and 0.1 M $TBABF_4$, $l = 0.5$ μm; (B and C) 1.5 mM $Os(bpy)_3^{2+}$ and 0.5 M KNO_3, $l = 1$ μm.

rate constants found from Figures 8D and 9D according to eq 12 are 0.12 cm/s for Fc^+ and 0.13 cm/s for $Os(bpy)_3^{3+}$. The actual rate constants may be significantly larger.

At small tip−substrate separations (e.g., $d/a \leq 2$) the radius of the portion of the substrate surface participating in the SECM feedback loop is of the same order of magnitude as the tip radius.[40] Thus, a large substrate facing the tip electrode behaves

as a virtual UME, and the current density for this portion of the substrate is comparable to the tip current density. To support a maximum current density of about 50 mA/cm^2 (Figure 9D), the effective diffusion coefficient for charge transport in reduced PPy (from thin-layer theory, assuming the concentration of charge carriers in reduced PPy as high as 0.1 M) should be at least 5×10^{-6} cm^2/s, in sharp contrast with the D values on the order of $10^{-10}-10^{-9}$ cm^2/s found by different authors for PPy in aqueous solutions and acetonitrile.[10,19,41] Thus, the interfacial redox reaction at a reduced PPy film is not accompanied by charge transport across the film, so that the $I_{T,max}$ value was independent of l. Anions should be ejected from the film or cations injected into it to maintain electroneutrality. Probably a small local region of oxidized (conductive) PPy is formed in this process. Such an island should grow with time so that eventually a significant portion of the film may become oxidized. Since the mediator regeneration was rapid at both reduced and oxidized PPy, we were unable to monitor the rate of this process by SECM. However, the current instabilities observed during the long-time (minutes) measurements with the tip positioned close to the reduced PPy film may have been caused by slow film oxidation. The islands of oxidized PPy could probably be imaged using a different redox mediator with a more negative standard potential (see below).

It is interesting to compare the above results to those obtained with a $Ru(NH_3)_6^{3/2+}$ mediator,[42] whose formal potential is much more negative, i.e., about −200 mV vs SCE. The tip and substrate processes were

$$Ru(NH_3)_6^{3+} + e^- = Ru(NH_3)_6^{2+} \text{ (tip)} \quad (13)$$

$$Ru(NH_3)_6^{2+} - e^- = Ru(NH_3)_6^{3+} \text{ (substrate)} \quad (14)$$

At $E_S \leq 0$ V vs SCE, the substrate appeared insulating because $Ru(NH_3)_6^{2+}$ cannot be oxidized chemically at a reduced PPy film, and electrochemical oxidation, although thermodynamically possible at $E_S \geq -0.2$ V vs SCE, did not occur because of high film resistance. The half-wave potential of the I_T-E_S curve (curve 1 in Figure 3A[42]), corresponding to $Ru(NH_3)_6^{2+}$ oxidation at oxidized PPy, was about +100 to +200 mV vs SCE, i.e., 300−400 mV more positive than the standard potential of the $Ru(NH_3)_6^{3/2+}$ couple. Although mediator regeneration in this case probably occurs via an electrochemical reaction as above (chemical oxidation of $Ru(NH_3)_6^{2+}$ may also contribute because of the higher concentration of oxidized moieties in oxidized PPy), the I_T-E_S curve reflects the change in conductivity during oxidation/reduction of PPy[39] rather than $Ru(NH_3)_6^{2+}$ electrochemistry. This is probably the origin of non-steady-state I_T-E_S curves obtained in ref 42 in contrast to ours.

Finally, we would like to comment on the determination of the electrochemical standard rate constant for et at the PPy/solution interface. Several such attempts have been reported beginning with the pioneering work of Diaz et al.[43] There are at least three reasons that data obtained by CV at large PPy-covered electrodes are not reliable: (1) the actual PPy surface is much larger than the apparent geometrical area of the modified electrode due to the film porosity and penetration of the redox species into the PPy layer, (2) the recorded CV always contains some contribution from PPy oxidation and reduction (i^{poly}) as well as charging current (i_{DL}) which cannot be separated or subtracted, and (3) adequate compensation of iR-drop in both the film and solution is not possible. Figure 10A provides some support for these generalizations. The peak separation on the substrate CV at $\nu = 20$ mV/s, $\Delta E_p = 87$ mV, is even larger than the one obtained in ref 43 at a 0.5-μm-thick PPy^+/BF_4^- film (75 mV), because we did not employ iR-compensation as used in ref 43. While the substrate current contains contributions from different Faradaic and non-Faradaic processes, the tip current represents only the turnover of the redox mediator, thus allowing one to separate the main redox reaction from parallel processes (i.e., the i_{DL}, i_{CT}, and i^{poly} components in eq 6) and to minimize iR-drop effects.[15,44] From the essentially steady-state I_T-E_S curve in Figure 10A, where the minor deviations from steady state are due to the depletion of mediator occurring at positive tip potentials that apparently did not affect the forward portion of the I_T-E_S curve, one can extract differences between quartile potentials as small as $|E_{1/2} - E_{1/4}| = 29$ mV and $|E_{3/4} - E_{1/2}| = 30$ mV. These correspond to essentially reversible et;[45] that is, the lower limit for the effective standard rate constant (calculated as $k^\circ \geq 10m$, where m is the mass-transfer coefficient[45]) is more than 1 cm/s. This value is much higher than $k^\circ = 0.04$ cm/s reported in ref 43. Moreover, the kinetics observed at thin PPy films ($l \ll 1$ μm) are probably associated with et at a metal substrate as well as at PPy itself. For $Os(bpy)_3^{3+/2+}$, the differences between quartile potentials, $|E_{1/2} - E_{1/4}| = 28$ mV and $|E_{3/4} - E_{1/2}| = 30$ mV, extracted from Figure 10B also correspond to an essentially Nernstian process. The lower limit for k° in this case is 0.2 cm/s. The separation of the main redox reaction from parallel processes is most apparent in this figure, where the I_T-E_S curve has the shape of a regular steady-state voltammogram, while the corresponding substrate CV is intractable.

Conclusions

The incorporation of cations, rather than expulsion of bromide anions, is the main ion transport process accompanying electrochemical reductions of PPy^+/Br^- and PPy^+/FCN^- at potentials less negative than −0.2 to −0.3 V vs SCE; anion ejection eventually occurs at more negative potentials. The incorporation of hexaammineruthenium(III) cations in PPy accompanying a potential step from +0.5 to 0 V vs SCE has been demonstrated for PPy doped with both small anions, like bromide, and large polyanions, such as poly(*p*-styrenesulfonate). These cations were released during a subsequent oxidation step and monitored with the help of the SECM tip electrode. $Fe(CN)_6^{4-}$ counterions seem to be strongly attached to a PPy film and only leave the film at more negative potentials and with a significant time delay. With TEA^+ cations in solution, two different kind of species are released from a PPy^+/FCN^- film, i.e., ferrocyanide anion itself and some apparently positive or neutral ferrocyanide-containing complex species ejected at $E_S \cong +50$ mV during PPy oxidation following a reduction cycle.

Electron transfer from PPy to Fc^+ and $Os(bpy)_3^{3+}$ species takes place within a thin (submicrometer-thick) layer adjacent to the film surface. Reduction of the oxidized form at an oxidized PPy film proceeds via an electrochemical reaction between solution species and the delocalized conduction band of PPy. The oxidized PPy in this case behaves as a porous metal rather than as a redox polymer. At reduced PPy, the solution species react chemically with individual PPy units. Although this picture is closer to a redox polymer model, a difference is the absence of charge transport across the film, with local ion ejection and incorporation being the mechanism of charge compensation. The essentially constant tip current in Figure 10C reflects the transition from an electrochemical regeneration of the mediator to a chemical one accompanying the reduction of the PPy film. Because both heterogeneous reactions are rapid under the conditions of our experiments, a quantitative distinction was not possible. For the apparent electrochemical standard rate constants, the lower limits are 1

cm/s ($Fc^{+/0}$) and 0.2 cm/s ($Os(bpy)_3^{3/2+}$); the lower limits for chemical heterogeneous rate constants are 0.12 cm/s (Fc^{+}) and 0.13 cm/s ($Os(bpy)_3^{3+}$).

Acknowledgment. The support of this research by grants from the National Science Foundation (CHE 9214480) and the Robert A. Welch Foundation is gratefully acknowledged. M.A. acknowledges financial support from the Islamic Development Bank Merit Scholarship Program. Our thanks to Ben Horrocks and Frank Fan for helpful discussions.

References and Notes

(1) (a) Murray, R. W. In *Electroanalytical Chemistry*; Bard, A. J., Ed.; Marcel Dekker: New York, 1984; Vol. 13, p 191. (b) Hillman, A. R. In *Electrochemical Science and Technology of Polymers*; Lindford, R. G., Ed.; Elsevier: London, 1987; p 103. (c) Inzelt, G. In *Electroanalytical Chemistry*; Bard, A. J., Ed.; Marcel Dekker: New York, 1994; Vol. 18, p 89.

(2) Novak, P.; Kötz, R.; Haas, O. *J. Electrochem. Soc.* **1993**, *140*, 37.

(3) John, R.; Wallace, G. G. *J. Electroanal. Chem.* **1993**, *354*, 145.

(4) Ren, X.; Pickup, P. G. *J. Phys. Chem.* **1993**, *97*, 5356.

(5) (a) Bose, C. S. C.; Basak, S.; Rajeshwar, K. *J. Phys. Chem.* **1992**, *96*, 9899. (b) Chen, C. C.; Wei, C.; Rajeshwar, K. *Anal. Chem.* **1993**, *65*, 2437.

(6) Kaufman, J. N.; Kanazawa, K. K.; Street, G. B. *Phys. Rev. Lett.* **1984**, *53*, 2461.

(7) Baker, C. K.; Qiu, Y.-J.; Reynolds, J. R. *J. Phys. Chem.* **1991**, *95*, 4446.

(8) Naoi, K.; Lien, M.; Smyrl, W. H. *J. Electrochem. Soc.* **1991**, *138*, 440.

(9) Heinze, J.; Bilger, R. *Ber. Bunsen-Ges. Phys. Chem.* **1993**, *97*, 502.

(10) Lee, C.; Kwak, J.; Bard, A. J. *J. Electrochem. Soc.* **1989**, *136*, 3720.

(11) Pei, Q.; Inganäs, O. *J. Phys. Chem.* **1992**, *96*, 10507.

(12) Kwak, J.; Anson, F. C. *Anal. Chem.* **1992**, *64*, 250. Lee, C.; Anson, F. C. *Anal. Chem.* **1992**, *64*, 528.

(13) (a) Denuault, G.; Trise Frank, M. H.; Peter, L. M. *Faraday Discuss.* **1992**, *94*, 23. (b) Trise Frank, M. H.; Denuault, G. *J. Electroanal. Chem.* **1993**, *354*, 331.

(14) Buttry, D. A.; Ward, M. D. *Chem. Rev.* **1992**, *92*, 1355.

(15) For recent reviews of SECM, see: Bard, A. J.; Fan, F.-R. F.; Mirkin, M. V. In *Electroanalytical Chemistry*; Bard, A. J., Ed.; Marcel Dekker: New York, 1994; Vol. 18, p 243. Bard, A. J.; Fan, F.-R. F.; Mirkin, M. V. In *Physical Electrochemistry: Principles, Methods and Applications*; Rubinstein, I., Ed.; Marcel Dekker: New York, in press.

(16) Diaz, A. F.; Castillo, J. I. *J. Chem. Soc., Chem. Commun.* **1980**, 397.

(17) Bull, R. A.; Fan, F.-R. F.; Bard, A. J. *J. Electrochem. Soc.* **1982**, *129*, 1009.

(18) Feldberg, S. W. *J. Am. Chem. Soc.* **1984**, *106*, 4671.

(19) Penner, R. M.; Martin, C. R. *J. Electrochem. Soc.* **1986**, *133*, 310. Penner, R. M.; Martin, C. R. *J. Phys. Chem.* **1989**, *93*, 984.

(20) Albery, W. J.; Chen, Z.; Horrocks, B. R.; Mount, A. R.; Wilson, P. J.; Bloor, D.; Monkman, A. T.; Elliott, C. M. *Faraday Discuss. Chem. Soc.* **1989**, *88*, 247. Albery, W. J.; Elliott, C. M.; Mount, A. R. *J. Electroanal. Chem.* **1990**, *288*, 15. Albery, W. J.; Mount, A. R. *J. Electroanal. Chem.* **1991**, *305*, 3.

(21) Li, F.; Albery, W. J. *J. Chem. Soc. Faraday Trans.* **1991**, *87*, 2949.

(22) Doblhofer, K. *J. Electroanal. Chem.* **1992**, *331*, 1015.

(23) Amemiya, T.; Hashimoto, K.; Fujishima, A. *J. Phys. Chem.* **1993**, *97*, 9736.

(24) Aoki, K.; Tezuka, Y. *J. Electroanal. Chem.* **1989**, *267*, 55. Aoki, K. *J. Electroanal. Chem.* **1993**, *348*, 273.

(25) Abrantes, L. M.; Mesquita, J. C.; Kalaji, M.; Peter, L. M. *J. Electroanal. Chem.* **1991**, *307*, 275. Vuki, M.; Kalaji, M.; Nyholm, L.; Peter, L. M. *J. Electroanal. Chem.* **1992**, *332*, 315.

(26) Ren, X.; Pickup, P. G. *J. Phys. Chem.* **1993**, *97*, 3941.

(27) Vorotyntsev, M. A.; Daikhin, L. I.; Levi, M. D. *J. Electroanal. Chem.* **1992**, *332*, 213.

(28) Gaudiello, J. G.; Sharp, P. R.; Bard, A. J. *J. Am. Chem. Soc.* **1982**, *104*, 6373.

(29) Bard, A. J.; Fan, F.-R. F.; Kwak, J.; Lev, O. *Anal. Chem.* **1989**, *61*, 1794.

(30) Wipf, D. O.; Bard, A. J. *J. Electrochem. Soc.* **1991**, *138*, 496.

(31) Dong, S.; Lian, G. *J. Electroanal. Chem.* **1990**, *291*, 23.

(32) Horrocks, B. R.; Mirkin, M. V.; Pierce, D. T.; Bard, A. J.; Nagy, G.; Toth, K. *Anal. Chem.* **1993**, *65*, 1213.

(33) Mirkin, M. V.; Arca, M.; Bard, A. J. *J. Phys. Chem.* **1993**, *97*, 10790.

(34) Fan, F.-R. F.; Mirkin, M. V.; Bard, A. J. *J. Phys. Chem.* **1994**, *98*, 1475.

(35) Park, D.-S.; Shim, Y.-B.; Park, S.-M. *J. Electrochem. Soc.* **1993**, *140*, 2749 and references cited therein.

(36) Miller, L. L.; Zinger, B.; Zhou, Q.-X. *J. Am. Chem. Soc.* **1987**, *109*, 2267.

(37) Lewis, N. S. *Annu. Rev. Phys. Chem.* **1991**, *42*, 543.

(38) Kwak, J.; Bard, A. J. *Anal. Chem.* **1989**, *61*, 1221.

(39) Feldman, B. J.; Burgmayer, P.; Murray, R. W. *J. Am. Chem. Soc.* **1985**, *107*, 872.

(40) Bard, A. J.; Mirkin, M. V.; Unwin, P. R.; Wipf, D. O. *J. Phys. Chem.* **1992**, *96*, 1861.

(41) Genies, E. M.; Bidan, G.; Diaz, A. F. *J. Electroanal. Chem.* **1983**, *149*, 101.

(42) Kwak, J.; Lee, C.; Bard, A. J. *J. Electrochem. Soc.* **1990**, *137*, 1481.

(43) Diaz, A.; Vallejo, J. M. V.; Duran, A. M. *IBM J. Res. Develop.* **1981**, *25*, 42.

(44) Horrocks, B. R.; Mirkin, M. V.; Bard, A. J. *J. Phys. Chem.* **1994**, *98*, 9106.

(45) Mirkin, M. V.; Bard, A. J. *Anal. Chem.* **1992**, *64*, 2293.

JP941389D